



HAL
open science

Generalized framework for adjoint error estimation of PG method in linear problems

Stefano d'Angelo, Mario Ricchiuto, Remi Abgrall, Herman Deconinck

► **To cite this version:**

Stefano d'Angelo, Mario Ricchiuto, Remi Abgrall, Herman Deconinck. Generalized framework for adjoint error estimation of PG method in linear problems. [Research Report] RR-7613, 2011. inria-00591666v4

HAL Id: inria-00591666

<https://inria.hal.science/inria-00591666v4>

Submitted on 28 Aug 2011 (v4), last revised 19 Dec 2011 (v5)

HAL is a multi-disciplinary open access archive for the deposit and dissemination of scientific research documents, whether they are published or not. The documents may come from teaching and research institutions in France or abroad, or from public or private research centers.

L'archive ouverte pluridisciplinaire **HAL**, est destinée au dépôt et à la diffusion de documents scientifiques de niveau recherche, publiés ou non, émanant des établissements d'enseignement et de recherche français ou étrangers, des laboratoires publics ou privés.

*Generalized framework for
adjoint error estimation of
PG method in linear problems*

S. D'Angelo — M. Ricchiuto — R. Abgrall — H. Deconinck

N° 7613

May 2011

Thème NUM



*Rapport
de recherche*

Generalized framework for adjoint error estimation of PG method in linear problems

S. D'Angelo*, M. Ricchiuto[†], R. Abgrall[‡], H. Deconinck[§]

Thème NUM — Systèmes numériques
Équipes-Projets BACCHUS

Rapport de recherche n° 7613 — May 2011 — 18 pages

Abstract: The current work concerns the study and the implementation of a modern algorithm for error estimation in CFD computations. This estimate involves the dealing of the adjoint argument. By solving the adjoint problem, it is possible to obtain important information about the transport of the error towards the quantity of interest. The aim is to apply for the first time this procedure into Petrov-Galerkin (PG) method. Streamline Upwind Petrov-Galerkin, stabilised Residual Distribution and bubble method are involved for the implementation. Scalar linear hyperbolic problems are used as test cases.

Key-words: Error Estimation, adjoint problem, Petrov-Galerkin method, Residual Distribution scheme, advection-reaction problem

* Aeronautics and aerospace department, von Karman Institute for Fluid Dynamics, Belgium

[†] INRIA Bordeaux Sud-Ouest, Equipe BACCHUS

[‡] INRIA Bordeaux Sud-Ouest, Equipe BACCHUS

[§] Aeronautics and aerospace department, von Karman Institute for Fluid Dynamics, Belgium

Generalized framework for adjoint error estimation of PG method in linear problems

Résumé : The current work concerns the study and the implementation of a modern algorithm for error estimation in CFD computations. This estimate involves the dealing of the adjoint argument. By solving the adjoint problem, it is possible to obtain important information about the transport of the error towards the quantity of interest. The aim is to apply for the first time this procedure into Petrov-Galerkin (PG) method. Streamline Upwind Petrov-Galerkin, stabilised Residual Distribution and bubble method are involved for the implementation. Scalar linear hyperbolic problems are used as test cases.

Mots-clés : Error Estimation, adjoint problem, Petrov-Galerkin method, Residual Distribution scheme, advection-reaction problem

Contents

1	Introduction	3
2	Definition in continuous	4
2.1	Linear advection-reaction	5
3	Numerical discretization	6
3.1	Broken space $\mathcal{V}_{h,q}^B$	7
3.2	Numerical analysis	7
4	Error Representation Formula	10
5	Numerical Results	13
6	Open questions and summary	17
7	Conclusions	17
A	Strong boundary conditions	17

1 Introduction

Over the last decade, much progress has been made in the area of Error Estimation. This theory provides a way to construct error indicators for CFD computations of PDE's. These error indicators can be used to drive automatic mesh adaptation algorithms. By adapting the mesh, we optimize the mesh spacings or reduce memory usage.

In this field, the *a posteriori* error analysis is one of the most used procedures to compute numerical error indicators. The relevance and generality of this estimation has been powerfully argued in the work of Johnson and his collaborators [1]. The *a posteriori* error bounds resulting from this analysis involve the numerical residual, obtained by inserting the computed solution into the current problem equations; this residual measures the extent to which the numerical approximation to the analytical solution fails to satisfy the current problem. From this study, the *Type II a posteriori* error bounds have been defined.

Becker and Rannacher worked also on this issue and they developed the so-called weighted-residual-based, or *Type I, a posteriori* error estimation ([2] and [3]). Here, the error representation formula defines the error in the target functional with the numerical residual, weighted by the solution of an adjoint problem. The key ingredient is this auxiliary problem, involving the formal adjoint of the current partial differential operator. For computing this product, also this adjoint problem will have to be implemented and solved numerically. For solving the adjoint problem, added cost rises. However, it is paid back by important information which helps us to identify where the real source of the error comes from. For example, Hartmann ([4]) shows the relevance and the advantages of *Type I* indicators over the *Type II* for the adaptive mesh design for a supersonic flow past an airfoil.

The data for the adjoint problem is a quantity of interest depending on the application. In engineering applications, this is typically a functional of the analytical solution such as a mean, point value, boundary flux. In fluid dynamics, it may be the pression at

the stagnation point, the pressure-drop between inflow and outflow or the drag or lift coefficients of a body immersed into the fluid.

2 Definition in continuous

Primal problem model: Let Ω be a bounded open domain R^d with boundary Γ . Given the *primal problem*

$$Lu = f \quad \text{in } \Omega \qquad Bu = g \quad \text{on } \Gamma \qquad (1)$$

where $f \in L^2(\Omega)$ and $g \in L^2(\Gamma)$, L denotes a linear differential operator on Ω and B denotes a linear boundary operator on Γ .

To solve this problem a numerical discretization is given and an approximated solution, u_h , is sought in the place of u , by using a discrete numerical method. We consider the numerical solution as a linear combination of piecewise polynomial functions of degree p on a partition \mathcal{T}_h of the domain Ω . For this reason we can write $u_h \in V_{h,p}$.

The functional $J(\cdot)$: In many problems of physical interest the quantity of interest for the current problem is an output or target functional of the solution rather the solution itself. This target functional is defined as $J(\cdot)$. Depending on the problem, it can be a different quantity, for example the drag or the lift coefficient or a point value of the solution.

This functional will be computed numerically and evaluated by the numerical solution, $J_h(u_h)$. The final purpose is to compute as good as possible this quantity, trying to estimate the order of error that the numerical approximations generate. Given a tolerance $\text{TOL} > 0$, then the problem might be defined as finding $u_h \in V_{h,p}$ such that

$$|J(u) - J_h(u_h)| \leq \text{TOL} \qquad (2)$$

Associated adjoint problem: Mathematical theory tells us that, by the (continuous) *compatibility condition*

$$(Lu, v)_\Omega + (Bu, C^*v)_\Gamma = (u, L^*v)_\Omega + (Cu, B^*v)_\Gamma \qquad (3)$$

for each operator appearing in the primal problem, L , B and C , there exists a corresponding adjoint one, L^* , B^* and C^* . By these so-called *adjoint operators*, we build the adjoint problem associated to (1)

$$L^*z = j_\Omega \quad \text{in } \Omega, \qquad B^*z = j_\Gamma \quad \text{on } \Gamma. \qquad (4)$$

Terms j_Ω and j_Γ on the right-hand side depend on the target quantity that we want to investigate and that, according to the theory, it is defined as follows

$$J(\omega) = (\omega, j_\Omega)_\Omega + (C\omega, j_\Gamma)_\Gamma \qquad (5)$$

where $j_\Omega \in L^2(\Omega)$ and $j_\Gamma \in L^2(\Gamma)$ and C is a differential boundary operator on Γ . The associated adjoint problem is hugely important. It provides how the information is

transported towards the current quantity of interest. This property is extremely useful to derive where and how the source of the error of the target quantity is carried over the domain. The error indicator derived by this further information will be able to refine only the terms that really affect the error of the quantity of interest.

2.1 Linear advection-reaction

Let consider the linear advection-reaction problem

$$\nabla \cdot (\mathbf{b}u) + cu = f \quad \text{in } \Omega \quad u = g \quad \text{on } \Gamma_- \quad (6)$$

where $f \in L^2(\Omega)$, $\mathbf{b} \in [C^1(\Omega)]^d$ and $\nabla \cdot \mathbf{b} = 0$, $c \in L^\infty(\Omega)$ and $g \in L^2(\Gamma_-)$, where

$$\Gamma_- = \{\mathbf{x} \in \Gamma, \quad \mathbf{b}(\mathbf{x}) \cdot \mathbf{n}(\mathbf{x}) < 0\}$$

denotes the inflow part of the boundary $\Gamma = \partial\Omega$.

So we find,

$$Lu = \nabla \cdot (\mathbf{b}u) + cu, \quad Bu = \delta_{\Gamma_-} u, \quad Cu = \delta_{\Gamma_+} u$$

where

$$\delta_{\Gamma_\pm} = \begin{cases} 1 & \text{if } \mathbf{x} \in \Gamma_\pm \\ 0 & \text{otherwise} \end{cases}$$

Then, the (continuous) compatible condition becomes

$$(\nabla \cdot (\mathbf{b}u) + cu, z)_\Omega + (\delta_{\Gamma_-} u, -\mathbf{b} \cdot \mathbf{n}z)_\Gamma = (u, -\mathbf{b} \cdot \nabla z + cz)_\Omega + (\delta_{\Gamma_+} u, \mathbf{b} \cdot \mathbf{n}z)_\Gamma$$

with a linear target functional (5), the continuous adjoint problem is thus given by

$$-\mathbf{b} \cdot \nabla z + cz = j_\Omega \quad \text{in } \Omega \quad \mathbf{b} \cdot \mathbf{n}z = j_\Gamma \quad \text{on } \Gamma_+ \quad (7)$$

so

$$L^*z = -\mathbf{b} \cdot \nabla z + cz, \quad B^*z = \delta_{\Gamma_+} \mathbf{b} \cdot \mathbf{n}z, \quad C^*z = -\delta_{\Gamma_-} \mathbf{b} \cdot \mathbf{n}z$$

As seen, depending on j_Ω and j_Γ definitions a different functional is taken. Typical examples used for linear hyperbolic problems are

- Outflow functional

$$J_{\text{out}}(u) = \int_{\Gamma} \delta_+(\mathbf{b} \cdot \mathbf{n}) \psi u \, dl$$

with ψ a enough smooth function.

- Solution average functional

$$J_{\text{ave}}(u) = \int_{\Omega} u \, d\mathbf{x}$$

- Mollified pointwise functional

$$J_{\text{mol}}(u) = \int_{\Omega} \psi(r_0; |\mathbf{x} - \mathbf{x}_0|) u \, d\mathbf{x}$$

$$\psi(r_0; |\mathbf{x} - \mathbf{x}_0|) = \begin{cases} 0 & r \geq r_0 \\ \frac{e^{1/(r^2/r_0^2-1)}}{2\pi \int_0^{r_0} e^{1/(\xi^2/r_0^2-1)} \xi \, d\xi} & r < r_0 \end{cases}$$

3 Numerical discretization

Let Ω be subdivided into shape-regular mesh $\mathcal{K} = \{\kappa\}$ consisting of elements κ . Let $\mathcal{V}_{h,p}$ be the standard finite element space of piecewise polynomials of complete degree p with C^0 continuity between elements

$$\mathcal{V}_{h,p} = \{v : v \in C^0(\Omega), v|_{\kappa} \in \mathcal{P}_p(\kappa), \forall \kappa \in \mathcal{K}\} \quad (8)$$

with $\mathcal{P}(\kappa)$ the space of polynomials of degree $\leq p$ defined on an element κ . Let then define a second space $\mathcal{V}_{h,q}^B$ which is the mesh dependent broken space of piecewise polynomials of complete degree q in each κ with no continuity between elements

$$\mathcal{V}_{h,q}^B = \{v : v|_{\kappa} \in \mathcal{P}_q(\kappa), \forall \kappa \in \mathcal{K}\} \quad (9)$$

Let discretize both problems and solve them numerically by using a *Petrov-Galerkin* (PG) method, where trial and test functions belong to $\mathcal{V}_{h,p}$ and $\mathcal{V}_{h,q}^B$, depending on the current problem.

According to (8) and (9), the boundary conditions are not included in the functional spaces and then, they are added and solved thorough the current problem. The approach with a strong formulation for the boundary conditions is hint in A.

Then following (3), the (discrete) compatibility condition holds as follows

$$\begin{aligned} & (Lu_h, v_b)_\Omega + (Bu_h, C^*v_b)_\Gamma \\ & = \\ & (u_h, L^*v_b)_\Omega + (Cu_h, B^*v_b)_\Gamma + \sum_k (H(u_h, \mathbf{n}), v_B^\dagger)_{\partial\kappa \setminus \Gamma} \end{aligned} \quad (10)$$

where $H(w_h, \mathbf{n})$ is the numerical flux over $\partial\kappa$, which is continuous because the $w_h \in \mathcal{V}_{h,p}$, \mathbf{n} is the outward normal along the element boundary and v_B^\dagger the outward traces of v_b over $\partial\kappa$.

So we can define a bilinear operator $\mathcal{B}(\cdot, \cdot)$ as

$$\mathcal{B}(u_h, v_b) = (Lu_h, v_b)_\Omega + (Bu_h, C^*v_b)_\Gamma \quad (11)$$

The (discrete) primal problem is then defined as

PRIMAL PROBLEM Find $u_h \in \mathcal{V}_{h,p}$ such that

$$\mathcal{B}(u_h, v_b) = F(v_b) \quad \forall v_b \in \mathcal{V}_{h,q}^B \quad (12)$$

while the corresponding adjoint problem is given by

ADJOINT PROBLEM Find $z_B \in \mathcal{V}_{h,q}^B$ such that

$$\mathcal{B}(w_h, z_B) = J(w_h) \quad \forall w_h \in \mathcal{V}_{h,p} \quad (13)$$

As we see, both problems use the same operator $\mathcal{B}(\cdot, \cdot)$ but in the primal one, the solution $u_h \in \mathcal{V}_{h,p}$ and the test function belongs to $\mathcal{V}_{h,q}^B$, while for the adjoint problem, the solution $z_B \in \mathcal{V}_{h,q}^B$ and the test function is taken from $\mathcal{V}_{h,p}$.

3.1 Broken space $\mathcal{V}_{h,q}^B$

A plethora of possible Broken spaces $\mathcal{V}_{h,q}^B$ are available. Herebelow let list the three Petrov-Galerkin spaces that will be taken into account for the next computations. Therefore, let remind that for a PG method, all of the broken spaces $\mathcal{V}_{h,q}^B$ can be always defined by a sum of two contributions

$$\mathcal{V}_{h,q}^B = \text{span}\{\Psi^0 + \Psi^1\}$$

where Ψ^0 is the "main" shape function of the space and Ψ^1 is a element stabilizer term.

Streamline Upwind Petrov-Galerkin method In case of a Streamline Upwind Petrov-Galerkin (SUPG) method, the broken space $\mathcal{V}_{h,q}^B$ is the same than $\mathcal{V}_{h,p}$ with still the addition of a stabilizer term

$$\mathcal{V}_{h,q}^B = \text{span}\{\varphi_i^q + \tau_\kappa \mathbf{b} \cdot \nabla \varphi_i^q\} \quad (14)$$

where τ_κ is usually the size of the element κ and φ_i^q the Lagrange interpolant polynomial of the degree of freedom, i , and order q ; while, finally, \mathbf{b} is the local advection of the current problem. So for this functional space $\Psi_j^0 = \varphi_j^q$ and $\Psi_j^1 = \tau_\kappa \mathbf{b} \cdot \nabla \varphi_j^q$.

Residual-Distribution Method If the stabilised Residual Distribution (RD) space is chosen, the broken space, $\mathcal{V}_{h,q}^B$, is defined as

$$\begin{aligned} \mathcal{V}_{h,q}^B &= \text{span}\{\chi^\kappa \beta_i^\kappa\} & \text{for } q = 1 \\ \mathcal{V}_{h,q}^B &= \text{span}\{\chi^\kappa \beta_i^\kappa + \tau_\kappa \mathbf{b} \cdot \nabla \varphi_i^q\} & \text{for } q > 1 \end{aligned} \quad (15)$$

where $\beta_i^\kappa \in C^0$, χ^κ is 1 in κ and 0 everywhere else, while τ_κ is usually the size of the element κ and φ_i^q the Lagrange interpolant polynomial of the degree of freedom, i , and order q . So $\Psi_j^0 = \chi^\kappa \beta_j^\kappa$ and $\Psi_j^1 = 0$ or $\tau_\kappa \mathbf{b} \cdot \nabla \varphi_j^q$.

"Bubble" method The "bubble" method comes out from the equivalence of the RD and SUPG method. Indeed, it takes the following broken space $\mathcal{V}_{h,q}^B$

$$\mathcal{V}_{h,q}^B = \text{span}\{\varphi_i^q + S^\kappa \alpha_i^\kappa\} \quad (16)$$

where φ_i^q the Lagrange interpolant polynomial of the degree of freedom, i , and order q , while S^κ is a bubble function null along $\partial\kappa$. In this case, it is either a linear bubble, unary in the barycentric point \mathbf{x}_g , or a cubic one, coming out from the product of the three vertex linear functions. Finally α_i^κ is given by $\alpha_i^\kappa = \beta_i - \phi_i$, where β_i is the corresponding RD basis function. Then here $\Psi_j^0 = \varphi_j^q$ and $\Psi_j^1 = S^\kappa \alpha_i^\kappa$.

3.2 Numerical analysis

Consistency and adjoint consistency All Petrov-Galerkin methods hold the *Galerkin orthogonality*

$$\mathcal{B}(u - u_h, v_b) = 0 \quad \forall v \in \mathcal{V}_{h,p}^b \quad (17)$$

which means that the discretization error $e = u - u_h$ is orthogonal (with respect to the bilinear form \mathcal{B}) to the discrete test space $\mathcal{V}_{h,p}^b$. Hence, because $v \in \mathcal{V}_{h,p}^b \subset \mathcal{V}$, we find

$$\mathcal{B}(u, v) = F(v) \quad \forall v \in \mathcal{V} \quad (18)$$

This proves that a PG method is a *consistent* discretization of the primal problem (1). Furthermore, a numerical discretization is called also *adjoint consistent* [?], if the exact solution $z \in \mathcal{V}$ to the adjoint problem (4) satisfies

$$\mathcal{B}(w, z) = J(w) \quad \forall w \in \mathcal{V} \quad (19)$$

In other words, if the discrete adjoint problem is a consistent discretization of the continuous adjoint problem. Motivated by the identity (10) and replcing z_B by the exact solution z and because $w_h \in \mathcal{V}_{h,p} \subset \mathcal{V}$, we can state that the bilinear form \mathcal{B} is also adjoint consistent.

Convergence (order of convergence) Let $u \in H^{p+1}(\Omega)$ and $u_h \in \mathcal{V}_{h,p}$ be the solutions to (18) and (1), respectively. Then,

$$\|u - u_h\|_{L^2(\Omega)} \leq Ch^{p+1} |u|_{H^{p+1}(\Omega)} \quad (20)$$

Let $p \geq 0$ and $\mathcal{V}_{h,p}^b$ be the broken finite element space defined in (9). Then, by $P_{h,p}^b$ we denote the L^2 -projection onto $\mathcal{V}_{h,p}^b$, i.e. given a $u \in L^2(\Omega)$ we define $P_{h,p}^b u \in \mathcal{V}_{h,p}^b$ by

$$\int_{\Omega} (u - P_{h,p}^b u) v_h \, d\mathbf{x} = 0 \quad \forall v_h \in \mathcal{V}_{h,p}^b$$

we use the short notation $P_h u$ instead of $P_{h,p}^b u$ when is clear which projection is meant. Now, let $p \geq 0$ and $P_h v$ be the L^2 -projection. Suppose $v \in H^{p+1}(\Omega)$, then

$$\|v - P_h v\|_{H^{p+1}(\Omega)} \leq Ch \|v\|_{L^2(\Omega)} \quad (21)$$

To numerically verify the convergence rate for smooth primal and adjoint data, numerical solutions of the following 2-D advection problem [5] were obtained

$$\begin{aligned} \mathbf{b} \cdot \nabla u &= 0 & \text{in } \Omega \\ u &= g & \text{on } \Gamma \end{aligned} \quad (22)$$

with circular advection field $\mathbf{b} = (-y, x)$ and

$$g(x) = \begin{cases} \tilde{\psi}(9/20; |x - 1/2|)(1 - \tilde{\psi}(9/20; |x - 1/20|)) & y = 0, x \leq 1/2 \\ \tilde{\psi}(9/20; |x - 1/2|)(1 - \tilde{\psi}(9/20; |x - 19/20|)) & y = 0, x > 1/2 \\ 0 & \text{otherwise} \end{cases}$$

where $\tilde{\psi}(\cdot; \cdot)$ is a C^∞ function

$$\tilde{\psi}(r_0; r) = \begin{cases} 0 & r \geq r_0 \\ e^{1/(r^2/(r^2 - r_0^2))} & r < r_0 \end{cases}$$

The target quantity is the weighted outflow flux functional

$$J(u) = \int_0^1 \delta_+(\mathbf{b} \cdot \mathbf{n}) \psi_{\text{outflow}} u \, d\mathbf{x}$$

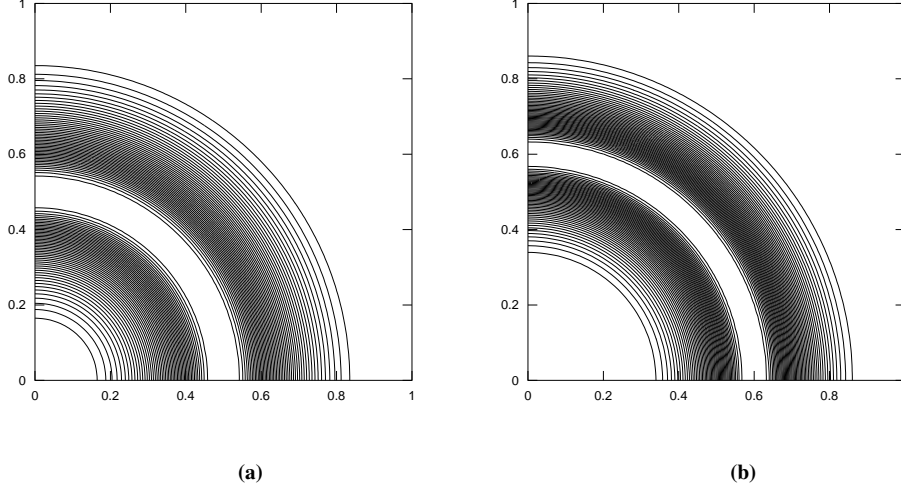


Figure 1: Barth's problem

with weighting function

$$\psi_{\text{outflow}}(y) = \begin{cases} \tilde{\psi}(7/20; |x - 3/5|)(1 - \tilde{\psi}(7/20; |x - 1/4|)) & x = 0, y \leq 3/5 \\ \tilde{\psi}(7/20; |x - 3/5|)(1 - \tilde{\psi}(7/20; |x - 19/20|)) & x = 0, y > 3/5 \\ 0 & \text{otherwise} \end{cases}$$

Figures 1a and 1b draw primal and adjoint current solutions, respectively, while table 1 tabulates values of the global solution error using a sequence of four nested meshes. Here, the $p + 1$ convergence rate for the u solution error is satisfied and so the rate for the adjoint solution. In this case, the latter rate is even better than the expected one from (25). The SUPG scheme keep the same convergence rate for both solutions, while the other schemes RD-LDA and BUBBLE show a order 2 for $p = 1$ and 1 for $p > 1$. Let now examine the convergence rates for functionals. We consider the general linear problem (1) and its numerical discretization (12), where the bilinear form $\mathcal{B}(\cdot, \cdot)$ is continuous on \mathcal{V} with respect to a specific $\|\cdot\|$ -norm, i.e.

$$\mathcal{B}(w, v) \leq C_B \|w\| \|v\| \quad \forall w, v \in \mathcal{V} \quad (23)$$

Because the discretization is consistent and thus, the Galerkin orthogonality is satisfied, we assume that following *a priori* error estimate in the $\|\cdot\|$ -norm holds: there are constants $C > 0$ and $r = r(p) > 0$ such that

$$\|u - u_h\| \leq Ch^r |u|_{H^{p+1}(\Omega)} \quad \forall u \in H^{p+1}(\Omega) \quad (24)$$

Finally, we assume that the projection operator $P_{h,p}^b$ satisfies following approximation estimate in the $\|\cdot\|$ -norm: there are constants $C > 0$ such that

$$\|v - P_{h,p}^b v\| \leq Ch \|v\|_{L^2(\Omega)} \quad \forall v \in L^2(\Omega) \quad (25)$$

Let then assume that the target quantity as described in (5) with j_Ω and j_Γ smooth functions on Ω and Γ , respectively. Then we have following estimate

$$\begin{aligned} |J(u) - J(u_h)| &= |\mathcal{B}(u - u_h, z)| = |\mathcal{B}(u - u_h, z - P_{h,p}^b z)| \\ &\leq Ch^{r+1} \|u\|_{H^{r+1}(\Omega)} \|v\|_{L^2(\Omega)} \end{aligned} \quad (26)$$

Once again, to numerically verify the convergence rate of functionals for a Petrov-Galerkin scheme let consider the circular advection problem [5] whose results are tabulated on table 1.

The $p + 1$ order for the functional error is satisfied by RD and BUBBLE schemes, while for SUPG a superconvergence rate $2p + 1$ is obtained. This behaviour seems to be strictly connected to the higher order of the corresponding adjoint solution of this scheme.

4 Error Representation Formula

Let consider the primal numerical problem (12) and that holds the *Galerkin orthogonality condition* (17). Let then notice that by the *compatibility condition* (3), using infinite-dimensional trial and test space, the adjoint problem can be redefined as

$$\mathcal{B}(w, z) = J(w) \quad \forall w \in \mathcal{V}$$

So, an exact error representation formula for a given functional $J(\cdot)$ results from the following steps, where P_h denotes any suitable projection operator (i.e. interpolation, L_2 projection) into $\mathcal{V}_{h,p}^b$,

$$\begin{aligned} J(u) - J(u_h) &= J(u - u_h) && \text{(linearity } J) \\ &= \mathcal{B}^*(z, u - u_h) && \text{(adjoint problem)} \\ &= \mathcal{B}(u - u_h, z) && \text{(compatibility condition)} \\ &= \mathcal{B}(u - u_h, z - P_h z) && \text{(orthogonality)} \\ &= \mathcal{B}(u, z - P_h z) - \mathcal{B}(u_h, z - P_h z) && \text{(linearity } \mathcal{B}) \\ &= F(z - P_h z) - \mathcal{B}(u_h, z - P_h z) && \text{(primal problem)} \end{aligned} \quad (27)$$

so in summary

$$J(u) - J(u_h) = F(z - P_h z) - \mathcal{B}(u_h, z - P_h z) \quad (28)$$

where no dependence on the exact solution u appears.

Computationally, this error representation formula is not suitable for obtaining computable *a posteriori* error estimation unless the function $z - P_h z$ is unknown, since $z \in \mathcal{V}^B$ is a solution of the infinite-dimensional adjoint problem. So z has to be computed by the discrete adjoint problem (13). Since the (10), we can solve the adjoint problem by using the same bilinear operator, $\mathcal{B}(w_h, z)$, used for the primal problem. Due to the Galerkin orthogonality, the adjoint numerical problem must be approximated in a larger space of functions than that utilized in the primal numerical problem. Here, this is achieved by solving the adjoint problem using a polynomial space that is one polynomial degree higher than the primal numerical problem, i.e. if $v_b \in \mathcal{V}_{h,q}^B$ then $z \approx z_{B'} \in \mathcal{V}_{h,q+1}^B$.

The error representation formula written in the global abstract form of the (28) does

Method	dofs	h	p	$\ u - u_h\ _{L^2}$	(rate)	$\ z - z_h\ _{L^2}$	(rate)	$ J(u) - J(u_h) $	(rate)
SUPG	1473	.0312	1	3.741e-03		5.239e-03		7.402e-05	
SUPG	5761	.0156	1	8.815e-04	(2.08)	1.839e-03	(1.51)	1.105e-05	(2.74)
SUPG	22785	.0078	1	1.552e-04	(2.50)	3.590e-04	(2.36)	1.438e-06	(2.94)
SUPG	90625	.0039	1	2.578e-05	(2.59)	6.275e-05	(2.52)	1.803e-07	(3.00)
RD-LDA	1473	.0312	1	3.675e-03		7.739e-03		2.188e-04	
RD-LDA	5761	.0156	1	1.092e-03	(1.75)	2.765e-03	(1.48)	5.968e-05	(1.87)
RD-LDA	22785	.0078	1	2.871e-04	(1.93)	7.869e-04	(1.81)	1.599e-05	(1.90)
RD-LDA	90625	.0039	1	7.335e-05	(1.97)	2.260e-04	(1.80)	4.128e-06	(1.95)
BUBBLE	1473	.0312	1	2.635e-03		4.661e-03		1.003e-04	
BUBBLE	5761	.0156	1	6.100e-04	(2.11)	1.492e-03	(1.64)	2.736e-05	(1.87)
BUBBLE	22785	.0078	1	1.472e-04	(2.05)	3.692e-04	(2.01)	7.201e-06	(1.93)
BUBBLE	90625	.0039	1	3.582e-05	(2.04)	1.011e-04	(1.87)	1.841e-06	(1.97)
SUPG	5761	.0312	2	2.624e-04		7.040e-04		5.785e-07	
SUPG	22785	.0156	2	3.243e-05	(3.01)	9.713e-05	(2.86)	2.236e-08	(4.69)
SUPG	90625	.0078	2	2.887e-06	(3.49)	1.057e-05	(3.20)	7.620e-10	(4.88)
SUPG	361473	.0039	2	3.138e-07	(3.20)	1.141e-06	(3.21)	2.412e-11	(4.98)
RD-LDA	5761	.0312	2	3.773e-04		8.681e-03		1.609e-06	
RD-LDA	22785	.0156	2	8.095e-05	(2.22)	4.951e-03	(0.81)	2.067e-07	(2.96)
RD-LDA	90625	.0078	2	1.544e-05	(2.39)	2.728e-03	(0.86)	2.869e-08	(2.85)
RD-LDA	361473	.0039	2	2.533e-06	(2.61)	1.481e-03	(0.88)	3.613e-09	(2.99)
BUBBLE	5761	.0312	2	1.806e-04		7.148e-03		3.907e-06	
BUBBLE	22785	.0156	2	3.800e-05	(2.25)	4.569e-03	(0.65)	6.089e-07	(2.68)
BUBBLE	90625	.0078	2	8.347e-06	(2.19)	2.720e-03	(0.75)	8.231e-08	(2.89)
BUBBLE	361473	.0039	2	1.645e-06	(2.34)	1.525e-03	(0.83)	1.063e-08	(2.95)

Table 1: Convergence rates of SUPG, RD and BUBBLE methods for circular advection problem [5].

not indicate which elements in the mesh should be refined to reduce the measured error in a functional. So, now the goal is to estimate the *local* contribution of each element in the mesh to the functional error. This local cell contribution will then be used as an error indicator for choosing which elements to refine or coarsen in the adaptive mesh procedure. By applying the *triangle inequality*, indeed, we have

$$\begin{aligned}
|J(u) - J(u_h)| &= |F(z - P_h z) - \mathcal{B}(u_h, z - P_h z)| && \text{(error representation)} \\
&= \left| \sum_{\kappa \in \mathcal{K}} F_\kappa(z - P_h z) - \mathcal{B}_\kappa(u_h, z - P_h z) \right| && \text{(element assembly)} \\
&\leq \sum_{\kappa \in \mathcal{K}} |F_\kappa(z - P_h z) - \mathcal{B}_\kappa(u_h, z - P_h z)| && \text{(triangle inequality)}
\end{aligned} \tag{29}$$

where

$$\begin{aligned}
F_\kappa(z - P_h z) - \mathcal{B}_\kappa(u_h, z - P_h z) &= (f - Lu, z - P_h z)_\kappa + (g - Bu, C^*(z - P_h z))_{\partial\kappa \cap \Gamma} \\
&= \mathcal{R}_\kappa(u_h, z - P_h z)
\end{aligned}$$

and

$$\mathcal{R}_\kappa(u, v) = (R(u), v)_\kappa + (r(u), C^*v)_{\partial\kappa \cap \Gamma}$$

with $R(u) = f - Lu$ and $r(u) = g - Bu$.

Adaptive Meshing : This direct estimate let us define for each partition element κ the *adaptation element indicator* η_κ

$$|\eta_\kappa| \equiv |\mathcal{R}_\kappa(u_h, z - P_h z)| \tag{30}$$

such that the simplest adaptation stopping criteria will be

$$|J(u) - J(u_h)| = \left| \sum_{\kappa} \eta_\kappa \right|$$

Hence, a simple mesh adaptation strategy can be outlined as follows:

1. Construct an initial mesh \mathcal{K}
2. Compute the numerical approximation of the primal problem on the current mesh \mathcal{K}
3. Compute the numerical approximation of the adjoint problem on the current mesh \mathcal{K}
4. Compute error indicators, η_κ , for all elements $\kappa \in \mathcal{K}$
5. If $|\sum_{\kappa \in \mathcal{K}} \eta_\kappa| < \text{TOL}$ where TOL is a given tolerance, then STOP
6. Otherwise, refine and coarsen a specified fraction of the total number of elements according to the size of $|\eta_\kappa|$, generate a new mesh \mathcal{K} and GOTO 2

5 Numerical Results

In this section, selected numerical examples are given for scalar advection (and/or reaction) problems. SUPG, RD and bubble schemes are the numerical schemes used for all cases. The following tables tabulate values of the functional error and the estimated error as given in (29) using numerically approximated adjoint problems.

In addition, an effectivity index is included to characterize the sharpness of the current estimates

$$\theta_{\text{eff}} = \frac{|\text{estimated error}|}{|J(u) - J(u_h)|} \quad (31)$$

When the exact adjoint solution is used

$$|J(u) - J(u_h)| = \left| \sum_{\kappa \in \mathcal{K}} \eta_{\kappa} \right| \equiv |\mathcal{E}_{\Omega}|$$

so the corresponding column in the following tables measures the effect of numerically approximating the adjoint problem. After application of the triangle inequality, the estimate

$$|J(u) - J(u_h)| \leq \sum_{\kappa \in \mathcal{K}} |\eta_{\kappa}| \equiv \mathcal{E}_{|\Omega|}$$

is obtained. Mesh adaptation strategies are usually based on $|\eta_{\kappa}|$ and so they depend on this error estimation. As internal cancellations are precluded, the estimate can usually lose in accuracy. Hence, column eight and nine of the following tables show the current estimate and its efficiency index.

Circular advection : The circular advection problem given in [5] is again considered. As we have already seen, both primal and adjoint solutions are enough smooth functions and then, their corresponding convergence rate (1) follows the theoretical rate. The smoothness condition leads also the first error estimation ($|\mathcal{E}_{\Omega}|$) to converge towards the exact functional error ($\theta_{\text{eff}} \approx 1$ for all schemes) and also to hold the second estimate ($\mathcal{E}_{|\Omega|}$), where only the RD with $p_p = 2$ and $p_a = 3$ gives θ_{eff} bigger than 10.

Advection-reaction : The advection-reaction case is defined by the following linear equation

$$\begin{aligned} \mathbf{b} \cdot \nabla u + cu &= f & \text{in } \Omega \\ u &= g & \text{on } \Gamma_- \end{aligned} \quad (32)$$

with $\mathbf{b} = (1, 0)$, $c = 1 - \text{sign}(x)x$. The source term f is given such that the analytical solution u^* of (32) is as follows

$$u^* = \alpha e^{-[a(x-x_0)^2 + b(y-y_0)^2]}$$

Finally, boundary conditions are consistent by the analytical solution. Once again the target quantity is an outflow functional such that the corresponding adjoint problem becomes

$$\begin{aligned} \mathbf{b} \cdot \nabla z + cz &= 0 & \text{in } \Omega \\ z &= 1 & \text{on } \Gamma_+ \end{aligned}$$

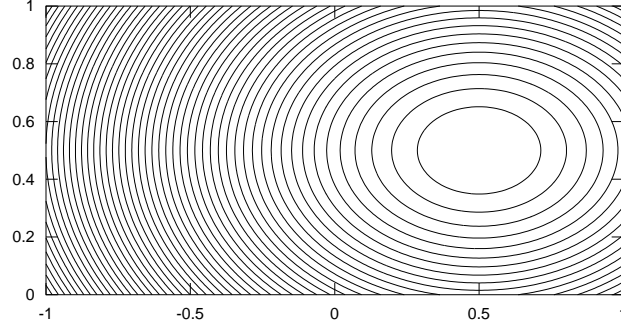
Figures 2a and 2b show primal and adjoint solutions, respectively, while error estimation data are tabulated on table 3. Here, RD-LDA scheme seem to be the best scheme. with all estimates which keep close to exact functional error. What sounds weird is the $p = 1$ SUPG estimate which seems out of control. This becomes even more weird by looking to the $p = 2$ estimate where both thetas converge to one.

Method	dofs	h	p_p	p_a	$ J(u) - J(u_h) $	$ \sum_{\kappa} \eta_{\kappa} $	(θ_{eff})	$\sum_{\kappa} \eta_{\kappa} $	(θ_{eff})
SUPG	1473	.0312	1	2	7.402e-05	7.402e-05	(1.00)	1.604e-04	(2.17)
SUPG	5761	.0156	1	2	1.105e-05	1.106e-05	(1.00)	2.231e-05	(2.02)
SUPG	22785	.0078	1	2	1.438e-06	1.439e-06	(1.00)	2.829e-06	(1.97)
SUPG	90625	.0039	1	2	1.803e-07	1.804e-07	(1.00)	3.538e-07	(1.96)
RD-LDA	1473	.0312	1	2	2.188e-04	2.202e-04	(1.01)	5.445e-04	(2.49)
RD-LDA	5761	.0156	1	2	5.968e-05	5.974e-05	(1.00)	1.321e-04	(2.21)
RD-LDA	22785	.0078	1	2	1.599e-05	1.599e-05	(1.00)	3.306e-05	(2.07)
RD-LDA	90625	.0039	1	2	4.128e-06	4.128e-06	(1.00)	8.234e-06	(2.00)
BUBBLE	1473	.0312	1	2	1.003e-04	1.032e-04	(1.03)	2.490e-04	(2.48)
BUBBLE	5761	.0156	1	2	2.736e-05	2.786e-05	(1.02)	6.089e-05	(2.23)
BUBBLE	22785	.0078	1	2	7.201e-06	7.266e-06	(1.01)	1.514e-05	(2.10)
BUBBLE	90625	.0039	1	2	1.841e-06	1.849e-06	(1.00)	3.740e-06	(2.03)
SUPG	5761	.0312	2	3	5.785e-07	5.727e-07	(.990)	9.610e-07	(1.66)
SUPG	22785	.0156	2	3	2.236e-08	2.237e-08	(1.00)	3.826e-08	(1.71)
SUPG	90625	.0078	2	3	7.620e-10	7.628e-10	(1.00)	1.340e-09	(1.76)
SUPG	361473	.0039	2	3	2.412e-11	2.441e-11	(1.01)	4.359e-11	(1.81)
RD-LDA	5761	.0312	2	3	1.609e-06	1.601e-06	(.995)	1.890e-05	(11.7)
RD-LDA	22785	.0156	2	3	2.067e-07	2.154e-07	(1.04)	3.037e-06	(14.7)
RD-LDA	90625	.0078	2	3	2.869e-08	2.937e-08	(1.02)	4.393e-07	(15.3)
RD-LDA	361473	.0039	2	3	3.613e-09	3.659e-09	(1.01)	5.961e-08	(16.5)
BUBBLE	5761	.0312	2	3	3.907e-06	3.997e-06	(1.02)	8.059e-06	(2.06)
BUBBLE	22785	.0156	2	3	6.089e-07	6.140e-07	(1.01)	1.300e-06	(2.14)
BUBBLE	90625	.0078	2	3	8.231e-08	8.267e-08	(1.00)	2.370e-07	(2.88)
BUBBLE	361473	.0039	2	3	1.063e-08	1.066e-08	(1.00)	3.907e-08	(3.67)

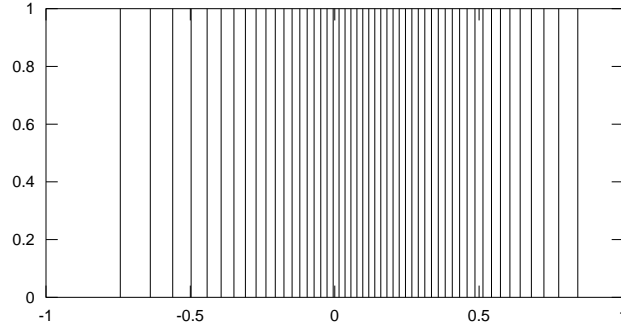
Table 2: Efficiency rates of the SUPG, RD and BUBBLE methods error estimates for the circular advection problem [5].

Method	dofs	h	p_p	p_a	$ J(u) - J(u_h) $	$ \sum_{\kappa} \eta_{\kappa} $	(θ_{eff})	$\sum_{\kappa} \eta_{\kappa} $	(θ_{eff})
SUPG	657	.0625	1	2	4.497e-07	1.247e-07	(.277)	8.753e-06	(19.5)
SUPG	2529	.0312	1	2	4.903e-08	8.227e-08	(1.68)	1.793e-06	(36.6)
SUPG	9921	.0156	1	2	5.465e-09	1.517e-08	(2.78)	4.015e-07	(73.5)
SUPG	39297	.0078	1	2	6.322e-10	2.211e-09	(3.50)	9.448e-08	(149)
RD-LDA	657	.0625	1	2	2.378e-05	2.502e-05	(1.05)	2.599e-05	(1.04)
RD-LDA	2529	.0312	1	2	5.955e-06	6.341e-06	(1.07)	6.601e-06	(1.11)
RD-LDA	9921	.0156	1	2	1.491e-06	1.598e-06	(1.07)	1.662e-06	(1.12)
RD-LDA	39297	.0078	1	2	3.731e-07	4.011e-07	(1.08)	4.170e-07	(1.12)
BUBBLE	657	.0625	1	2	5.918e-06	9.453e-06	(1.60)	1.000e-05	(1.69)
BUBBLE	2529	.0312	1	2	1.456e-06	2.197e-06	(1.51)	2.330e-06	(1.60)
BUBBLE	9921	.0156	1	2	3.610e-07	5.292e-07	(1.47)	5.613e-07	(1.56)
BUBBLE	39297	.0078	1	2	8.988e-08	1.298e-07	(1.45)	1.376e-07	(1.53)
SUPG	2529	.0625	2	3	7.432e-08	6.588e-08	(.886)	9.519e-08	(1.28)
SUPG	5761	.0312	2	3	1.012e-08	9.450e-09	(.934)	1.233e-08	(1.22)
SUPG	22785	.0156	2	3	1.318e-09	1.270e-09	(.964)	1.567e-09	(1.19)
SUPG	156417	.0078	2	3	1.679e-10	1.648e-10	(.981)	1.973e-10	(1.18)
RD-LDA	2529	.0625	2	3	2.087e-08	1.705e-08	(.817)	3.007e-08	(1.44)
RD-LDA	9921	.0312	2	3	2.604e-09	2.419e-09	(.929)	3.738e-09	(1.44)
RD-LDA	22785	.0156	2	3	3.214e-10	3.189e-10	(.992)	4.709e-10	(1.47)
RD-LDA	156417	.0078	2	3	3.968e-11	4.071e-11	(1.03)	5.895e-11	(1.49)
BUBBLE	2529	.0625	2	3	1.331e-08	3.364e-08	(2.53)	3.688e-08	(2.77)
BUBBLE	9921	.0312	2	3	1.544e-09	4.676e-09	(3.03)	5.106e-09	(3.31)
BUBBLE	22785	.0156	2	3	1.828e-10	6.179e-10	(3.38)	6.729e-10	(3.68)
BUBBLE	156417	.0078	2	3	2.196e-11	7.928e-11	(3.61)	8.713e-11	(3.97)

Table 3: Efficiency rates of the SUPG, RD and BUBBLE methods error estimates for the advection reaction problem.



(a)



(b)

Figure 2: Reaction problem**Figure 3:** Analytical solution for primal problem

Adaptive mesh comparison : Let consider the following problem

$$\begin{aligned} \mathbf{b} \cdot \nabla u + cu &= f \quad \text{in } \Omega \\ u &= g \quad \text{on } \Gamma_- \end{aligned} \quad (33)$$

where $\mathbf{b} = (10y^2 - 12x + 1, 1 + y)$, $c = 0$ and $f = 0$, while the inflow boundary conditions

$$u(x, y) = \begin{cases} 0, & \text{for } x = 0, \quad 0.5 < y \leq 1 \\ 1, & \text{for } x = 0, \quad 0 < y \leq 0.5 \\ 1, & \text{for } 0 \leq x \leq 0.5, \quad y = 0 \\ 0, & \text{for } 0.5 < x \leq 1, \quad y = 0 \\ \sin^3(\pi y) & \text{for } x = 1, \quad 0 \leq y \leq 1 \end{cases}$$

The analytical solution is shown in figure 3. Let us suppose that the target quantity is the weighted normal flux $J_\psi(u)$ through the outflow edge of the square, where the

weight-function ψ is defined as

$$\psi(x) = \sin(\pi x/2) \quad \text{for } 0 \leq x \leq 1, \quad y = 1$$

Let compare an *ad-hoc* residual based refinement and the adaptive algorithm based on the adjoint solution. In figure (4) we show the final meshes. Here, the adaptation based only by the residual gives high refinements along both discontinuity, even though they do not give any contribution for the accuracy of the functional. Hence, the given tolerance $\text{TOL} = 5.0 \times 10^{-6}$ is achieved by the adjoint error adaptation with a way too smaller number of dofs.

Figure 4: Final adapted mesh for problem (33) with *ad-hoc* and adjoint adaptation

In figure 5 we show the performance of the current adaptive algorithm. By using a common initial mesh...blablabla

Figure 5: Performance of the adaptive algorithm with $\text{TOL} = 5.0 \times 10^{-6}$.

6 Open questions and summary

- Convergence rate for $z - z_B$ and norm of $V_{h,p}^B$ space
- SUPG p1 and BUBBLE p2 with reaction bad estimation

7 Conclusions

Among different types of error representation formula, we interested in Type I error indicator. Unlike Type II error bounds where the only local residual is taken into account, Type I involves also the solution of the associated adjoint problem. By it, we are able to obtain further information concerning the transport of the error of computing the quantity of interest.

For the first time, we want to develop this error analysis applied a Petrov-Galerkin numerical discretization by using methods like Streamline Upwind PG and bubble method. We implement this error estimation theory on a code. We start by simple scalar first-order hyperbolic problem (using for the primal solution both $p = 1$ and $p = 2$) to pass later to more complicated problems like the 2D compressible Euler equations.

A Strong boundary conditions

Strong boundary conditions are realized by considering an appropriate function (sub)space $\mathcal{V}_{h,p,0} \subset \mathcal{V}_{h,p}$ (or $\mathcal{V}_{B,q,0} \subset \mathcal{V}_{B,q}$) which incorporates directly the conditions on the boundary Γ . Then, the function spaces to search the primal and adjoint solutions that also include homogenous boundary conditions are, respectively,

$$\begin{aligned} \mathcal{V}_{h,p,0} &= \{v : v \in C^0(\Omega), v|_{\kappa} \in \mathcal{P}_p(\kappa), \forall \kappa \in \mathcal{K}, Bv = 0 \text{ on } \Gamma\} \\ \mathcal{V}_{h,q,0}^B &= \{v : v|_{\kappa} \in \mathcal{P}_q(\kappa), \forall \kappa \in \mathcal{K}, B^*v = 0 \text{ on } \Gamma\} \end{aligned} \quad (34)$$

and so the corresponding bilinear operator is given by

$$\mathcal{B}_0(u_{h,0}, v_b) = (u_{h,0}, L^* v_b)_{\Omega} + \sum_k (H(u_{h,0}, \mathbf{n}), v_B^+)_{\partial\kappa \setminus \Gamma}$$

For the realization of the inhomogeneous inflow boundary conditions, assume that $u_h = u_{h,0} + u_g$ with $u_g \in \mathcal{V}_{h,p}$ and such that $Bu_h = g$ on Γ ; since $Bu_{h,0}|_{\Gamma} = 0$, by definition, then $Bu_g = g$ on Γ . The same approach is taken for $z_B = z_{B,0} + z_{j\Gamma}$, with $z_{j\Gamma} \in \mathcal{V}_{h,q}$ and where $B^* z_B = \hat{j}_{\Gamma}$ and $B^* z_{B,0} = 0$ on Γ such that $B^* z_{j\Gamma} = \hat{j}_{\Gamma}$ on Γ .

Acknowledgements

Work started during a visit of the first author in Bordeaux, partly funded by the ERC ADDECCO, #226316. MR and RA were partly funded by the ERC ADDECCO, #226316

References

- [1] P. Hansbo K. Eriksson, D. Estep and C. Johnson. Introduction to adaptive methods for different equations. *Acta Numerica*, pages 105–158, 1995.
- [2] R. Becker and R. Rannacher. A feed-back approach to error control in finite element methods: basis analysis and examples. *Journal Numerical Mathematics*, 4:237–264, 1996.
- [3] R. Becker and R. Rannacher. An optimal control approach to a-posteriori error estimation in finite element methods. *Acta Numerica*, 10:1–102, 2001.
- [4] R. Hartmann. *Adaptive Finite Element Methods for the Compressible Euler Equations*. PhD thesis, Universität Heidelberg, 2002.
- [5] R. Hartmann. Numerical analysis of higher order discontinuous galerkin finite element methods. In *35th CFD VKI/ADIGMA*, 2008.
- [6] T. Barth. *A Posteriori* error estimation and mesh adaptivity for finite volume and finite element methods. Technical report, NASA Ames Research Center, 2002.



Centre de recherche INRIA Bordeaux – Sud Ouest
Domaine Universitaire - 351, cours de la Libération - 33405 Talence Cedex (France)

Centre de recherche INRIA Grenoble – Rhône-Alpes : 655, avenue de l'Europe - 38334 Montbonnot Saint-Ismier
Centre de recherche INRIA Lille – Nord Europe : Parc Scientifique de la Haute Borne - 40, avenue Halley - 59650 Villeneuve d'Ascq
Centre de recherche INRIA Nancy – Grand Est : LORIA, Technopôle de Nancy-Brabois - Campus scientifique
615, rue du Jardin Botanique - BP 101 - 54602 Villers-lès-Nancy Cedex
Centre de recherche INRIA Paris – Rocquencourt : Domaine de Voluceau - Rocquencourt - BP 105 - 78153 Le Chesnay Cedex
Centre de recherche INRIA Rennes – Bretagne Atlantique : IRISA, Campus universitaire de Beaulieu - 35042 Rennes Cedex
Centre de recherche INRIA Saclay – Île-de-France : Parc Orsay Université - ZAC des Vignes : 4, rue Jacques Monod - 91893 Orsay Cedex
Centre de recherche INRIA Sophia Antipolis – Méditerranée : 2004, route des Lucioles - BP 93 - 06902 Sophia Antipolis Cedex

Éditeur
INRIA - Domaine de Voluceau - Rocquencourt, BP 105 - 78153 Le Chesnay Cedex (France)
<http://www.inria.fr>
ISSN 0249-6399